

Mini review

Alpha-particle Counting and Spectrometry in a Primary Standardisation Laboratory

Stefaan Pommé* and Geodele Sibbens

European Commission, Joint Research Centre, Institute for Reference Materials and Measurements,
Retieseweg 111, B-2440 Geel, Belgium

* Corresponding author: Tel.: +32(0)1 45 71 289; fax +32(0)1 45 71 864;
E-mail: stefaan.pomme@ec.europa.eu.

Received: 09-07-2007

Abstract

This paper describes the application of alpha-particle counting at a defined low solid angle and of high-resolution alpha-particle spectrometry at IRMM. These techniques are used in the frame of primary standardisations of radioactive solutions or for the determination of nuclear decay data (alpha emission probabilities and energies, half-lives). Various technical aspects are discussed, such as source preparation, instrumentation, solid-angle calculations, peak shapes, fitting routines, bias of least-squares methods, off-line stability corrections, simulation of energy loss, uncertainties. The presented algorithms may also be useful for routine alpha-particle spectrometry, in particular for the assessment of its uncertainty budget.

Keywords: Alpha-particle counting, alpha-particle spectrometry

1. Introduction

The Institute for Reference Materials and Measurements (IRMM) of the European Commission harbours a laboratory specialised in the primary standardisation of radioactivity.¹ Over the years, this lab has constructed various precision instruments and developed advanced methods for the accurate measurement of activity, traceable to the SI units. This paper describes the application of alpha-particle counting at a defined low solid angle and of high-resolution alpha-particle spectrometry at IRMM. Whereas the application of these techniques at IRMM is rather specific, the problems and solutions involved with alpha-particle spectrometry are of a general nature and may be of use for laboratories that aim at other applications, such as the measurement of environmental samples. The paper will focus on solutions accomplished at IRMM, as more general review papers on alpha-particle spectrometry have been published by Bortels and recently by García-Toraño.^{2,3}

2. Counting at a Defined Solid Angle (DSA)

2.1. Principle

Alpha-particle counting at a defined low solid angle is amongst the most accurate primary standardisation

methods for alpha-emitting radionuclides.^{4–6} It has been applied in various standardisation exercises,^{7–9} but also in the frame of half-life determinations of long-lived radionuclides.^{10–13} Excellent control of the geometrical conditions of the set-up is an essential requirement to reach a state-of-the-art level of accuracy. This comprises different aspects, like the careful design and mechanical construction of different set-up parts, the accurate determination of distances and the evaluation of the solid angle subtended by the detector, the use of a detector with known detection efficiency, the production of thin and uniform sources on a flat substrate. In ideal conditions, the detection efficiency is obtained directly from the geometry factor, i.e. the ratio of the solid angle to 4π steradian.

Fig. 1 shows the scheme of a typical set-up, designed by Denecke et al. It's a reproducible assembly of a source chamber, distance tube with anti-scatter baffles and various coaxial flanges with lapped, parallel faces, maintained in position with centring rings and air tight by rubber vacuum rings. The radioactive source material is deposited on a flat substrate and centred around the symmetry axis of the circular diaphragm in front of the detector, i.e. a large PIPS (passivated implanted planar silicon) detector (up to 5000 mm²), with an ultra-thin window and 100% intrinsic detection efficiency.¹⁴ The air in the source chamber is evacuated using a turbomolecular pump and a dry membrane pump, to produce an oil-free vacuum of 10⁻³ Pa or less. Scattering effects and energy loss of the al-

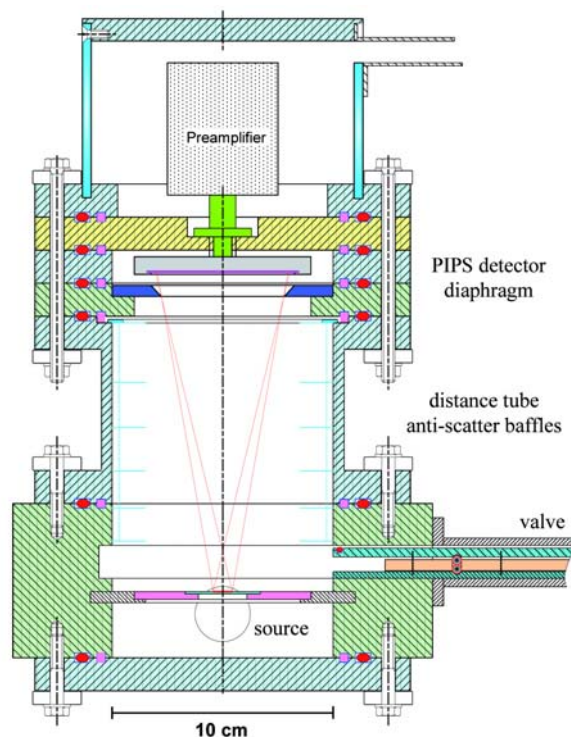


Fig. 1: Scheme of an alpha-particle counter with defined geometry, used for primary standardisation of activity.

pha particles in the source layer and the detector window are minimised by using a low solid angle, thus selecting the small fraction of alpha particles emitted rather perpendicular to the source.

One can correctly extrapolate the measured count rate to the total emission rate of the source by an accurate determination of the solid angle involved. The geometrical conditions should be measured with great accuracy, say within 10 microns, and in an SI-traceable manner (cf. *Système International d'unités*). The accuracy is limited on the source-to-diaphragm distance (due to uncertainty on the source substrate thickness) and on the position of the active material (due to source inhomogeneity and eccentricity). Solutions are thickness measurements by optical focussing of a travelling lens connected to a distance measuring device and autoradiography of the sources to determine the radial distribution of the activity on the substrate.¹⁵

The measured specific activity A [Bq g^{-1}] of a source with mass m [g] is calculated from the equation below:

$$A = \frac{R \cdot 4\pi}{\Omega \cdot \varepsilon \cdot m} \cdot f_{\text{corrections}}, \quad (1)$$

in which R is the count rate after correction for dead time, background and nuclear decay, Ω is the solid angle in ster-

dian, ε is the detector efficiency, $f_{\text{corrections}}$ is the combination of possible correction factors for counts below the discriminator threshold, self-absorption and scattering effects, interference from other radionuclides, material loss during source preparation, etc. A full uncertainty budget includes the propagation of all uncertainty components involved.

2. 2. Solid Angle

The problem of solid-angle calculation has been solved in different ways, including Monte Carlo simulations, analytical equations, series expansions,^{16–18} and, in particular a numerical integration method for an axially symmetric set-up with one or more diaphragms,^{15,19,20} including the possibility to take into account the true radial activity distribution of the source.^{15,21} The actual source can be represented by a set of coaxial annular rings with adjustable relative weights, corresponding to its radial activity distribution. Due to the axial symmetry, each point on the ring corresponds to a similar solid angle, and the overall solid angle is obtained from the weighted average of all rings.

A convenient, quickly converging formula for the solid angle subtended by a circular detector (radius R_D) for a co-axial, homogeneous, circular disk source (radius R_S , at distance h) follows from¹⁸:

$$\frac{\Omega}{4\pi} = \frac{R_D}{R_S} \frac{1}{2n} \sum_{i=1}^n \frac{\sin^2 \varphi}{\sqrt{x - \cos \varphi} (\sqrt{y + \sqrt{x - \cos \varphi}})} \quad (2)$$

$$\text{in which } x = \frac{R_S^2 + R_D^2 + h^2}{2R_S R_D}, \quad y = \frac{h^2}{2R_S R_D}$$

and $\varphi = (i-0.5)\pi/n$ and n is an integer value of choice (e.g. $n = 50$). The solid angle for an annular ring, Ω_{ring} , with inner radius R_{in} and outer radius R_{out} can be calculated from a linear combination of the solid angles Ω_{in} and Ω_{out} (Eq. 2) for two disk sources with radii R_{in} and R_{out} , respectively.¹⁵

$$\Omega_{\text{ring}} = \frac{R_{\text{out}}^2 \Omega_{\text{out}} - R_{\text{in}}^2 \Omega_{\text{in}}}{R_{\text{out}}^2 - R_{\text{in}}^2} \quad (3)$$

By varying the different geometrical parameters by their uncertainty, one can identify some major uncertainty components in alpha-particle counting efficiency. An example of an uncertainty budget in classical environmental alpha spectrometry was presented by Spasova et al.²²

2. 3. Other Correction Factors

Count loss due to system dead time is corrected for by a live-time clock where an accurately timed pulse train is counted only in those time intervals when the measur-

ing system is free to accept or record events.^{23,24} A stable quartz oscillator with a frequency of 100 Hz is used for this purpose. In order to control the type and duration of the characteristic dead time per recorded event, an extending or non-extending dead time is imposed that exceeds the pulse width of the detector signals and the recorded real-time to live-time ratio is used as correction factor for the incurred count loss. Additional pile-up cascade effects can be corrected for, but are usually low because of the relatively low count rates ($<10^3 \text{ s}^{-1}$) encountered in a low-solid-angle configuration.²⁹

The measurement duration and start time are registered in an SI-traceable manner, by comparing the clocks with the time and frequency standard produced by the primary atomic clocks of PTB (Physikalisch-Technische Bundesanstalt) in Braunschweig and transmitted via the DCF77 radio signal from Mainflingen, Germany.

The probability of counting scattered particles is low ($<0.01\%$), due to the low solid-angle configuration with thin, flat sources, vacuum and sharp edge diaphragm and baffles.⁴ There is no indication of significant scattering at the detector surface, or of a noticeable deviation from 100% efficiency. Low-energy backscattered particles and electronic noise are cut off by setting the low-level discriminator threshold above 1 MeV. The small fraction of counts lost ($<0.05\%$) below the threshold is compensated for by an extrapolation of the low-energy tail of the energy spectrum towards zero energy (see Fig 2). At the same time, this should compensate for the (low) probability of losing ‘self-absorbed’ particles.

Background count rates are usually very low ($\sim 10^{-3} \text{ s}^{-1}$) and can easily be subtracted from the source spectra. Contamination by recoiled α -emitters is avoided by covering the source with a thin VYNS (polyvinylchloride-polyvinylacetate copolymer) foil on a ring.²⁵ Possible impurities in the enriched material can be identified with high-

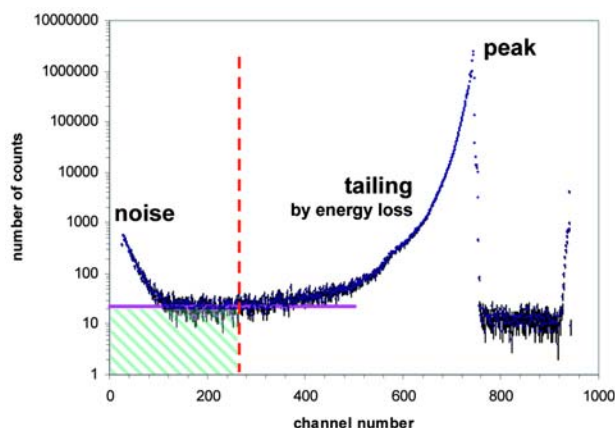


Fig. 2: ^{238}Pu α -spectrum with peak shift and distortion due to energy loss. Only counts above channel 250 are counted and the missing low-energy part is determined from an extrapolation to zero energy. Tailing is mainly caused by energy loss of alpha-particles via interaction with source material.

resolution α -particle or γ -ray spectrometry. Corrections for in-growth must be applied if any of the daughter nuclides emits α -particles, in particular if they cannot be distinguished from the parent decay. A decay correction factor is applied to adjust the measured rates to a reference date.

2. 4. Quantitative Source Preparation

As the method is used for standardisation of the activity of a radionuclide solution, sources are prepared by ‘drop deposition’ of accurately known aliquots of the solution, i.e. using a polyethylene pycnometer (see Fig. 3) to dispense droplets directly on a flat substrate (quartz, glass, silicon, stainless steel).^{26,27} The deposited amount is derived from two weighings of the pycnometer on a microbalance, calibrated with SI-traceable weights via the IRMM kilogram.²⁸

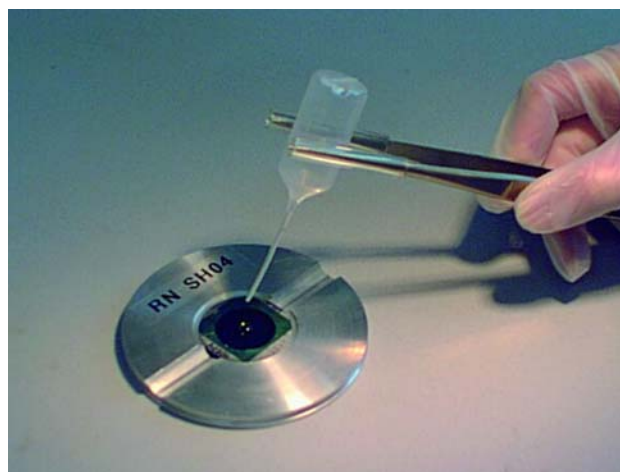


Fig. 3: Pycnometer dispensing aliquots of radioactive solution on a source substrate.



Fig. 4: IRMM’s drying device for drop-deposited radioactive sources, with control unit. The source is placed on a turntable and dried by the injection of heated nitrogen through four jets, inside a bell jar connected to a vacuum pump.

Special care is taken about the drying process. In order to reduce the probability for self-absorption in the solid source, the formation of agglomerates of big crystals has to be avoided. A more homogeneous spread of the active material is accomplished by adding a seeding and wetting agent to the droplet, and by accelerating the drying process with the IRMM source drying device (Fig. 4), i.e. by stirring the rotating source drop with multiple jets of dry nitrogen at elevated temperature.²⁹

2. 5. Simulation of Energy Loss

As self-absorption effects are difficult to estimate, computer simulations of energy loss may be useful. One may consider a simplified model where the energy loss of a particle with incidental energy E_0 (and range $R = E_0^{b+1}$, disregarding straggling effects) in a homogeneous layer with effective thickness $T = r/\cos\theta$ can be approximated by:³⁰

$$\Delta E = E_0 - {}^{b+1}\sqrt{E_0^{b+1} + T/a} \quad (4)$$

with parameters b and a as defined in Ref. 30.

The effective distance is corrected for the polar angle at which the particle is emitted. For a co-axial disk source and detector, the angular distribution can be calculated from:^{15,30}

$$\begin{cases} \left[\left(\frac{R_1}{R_S} \right)^2 2\pi + \frac{2}{R_S^2} \int_{R_1}^{R_2} 2(\pi - \varphi(r, \theta)) r dr \right] \sin \theta d\theta & \theta \in [0, \theta_1] \\ \frac{2}{R_S^2} \int_{R_0}^{R_2} 2(\pi - \varphi(r, \theta)) r dr \sin \theta d\theta & \theta \in [\theta_1, \theta_2] \end{cases} \quad (5)$$

in which the limits for the radius correspond to

$$\begin{cases} R_0 = d \tan \theta - R_D \\ R_1 = \min\{R_S, R_D - d \tan \theta\} \\ R_2 = \min\{R_S, R_D + d \tan \theta\} \end{cases}$$

and the limiting values for the angle are

$$\theta_1 \equiv \text{atan}\left(\frac{R_D}{d}\right) \text{ and } \theta_2 \equiv \text{atan}\left(\frac{R_D + R_S}{d}\right).$$

Applying this to a typical source, one gets too small energy loss effects. The simulations become more realistic by assuming that the radioactive material is concentrated in crystals rather than a perfectly thin homogeneous layer. In view of the axial symmetry, one can e.g. model the crystals as cones.

3. High-Resolution Alpha-particle Spectrometry

3. 1. Principle

Besides two DSA counters, IRMM has also two setups for high-resolution alpha-particle spectrometry, designed in collaboration with CIEMAT (Centro de Investigaciones Energéticas, Medioambientales y Tecnológicas, Spain). Fig. 5 shows a picture of such instrument, which shows quite some resemblance with a DSA counter. Unlike with the DSA counters, the primary aim is not to determine the activity, yet to obtain an energy spectrum of the emitted alpha particles with optimum resolution. Some specific differences are the presence of a thermostatic bath, vertically moveable source holder, smaller detector and magnet.



Fig. 5: Picture of set-up for high-resolution alpha-particle spectrometry.

PIPS detectors up to 5000 mm² can be mounted on a vacuum feedthrough (Microdot-connector) of the detector flange which is part of the preamplifier housing. For an optimum energy resolution, mainly small detectors are used. With a PIPS detector of 50 mm², one can reach 8.5 keV full width at half maximum resolution. For certain applications, a larger detector (e.g. 150 mm²) can be useful, because the tailing of a peak may be relatively lower at low energy side (see Fig. 6). The couple capacitor in the pre-amplifier is adapted to the detector capacity for noise reduction.

The detector flange and the preamplifier housing are temperature stabilised using the water circulation of a thermostatic bath, in order to minimise peak shift of the spectrum during the measurements. Room temperature is preferred, as cooling to lower temperatures can cause condensation of moisture on the detector with loss of resolution.

A port in the chamber allows changing the sources, by means of a slide. The source support is moveable in

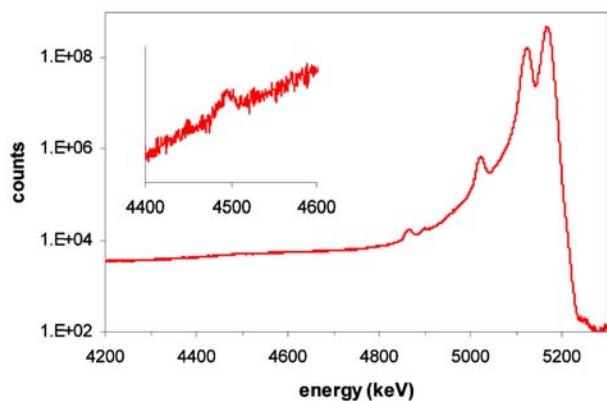


Fig. 6: ^{240}Pu spectrum showing small peaks on the tail of two main peaks, only visible with a relatively large detector of 150 mm².

vertical direction and the distance can be checked via a vernier calliper at the bottom. A sliding piston built on a vacuum feedthrough at the bottom flange allows to move the source continuously up to 100 mm closer to the detector. The top of the chamber is closed by a large shutter valve to confine the detector part of the system during source change. In this way detector operating conditions, e.g. bias and vacuum, are maintained. An electron bending magnet and diaphragm can be inserted between the

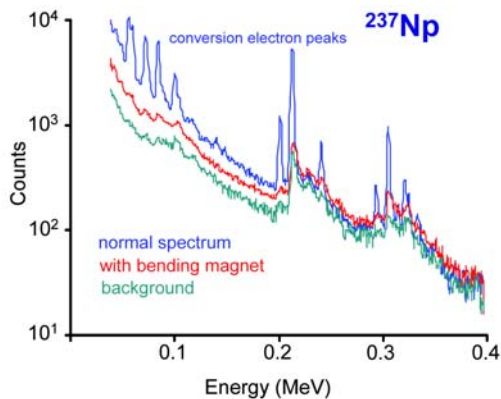
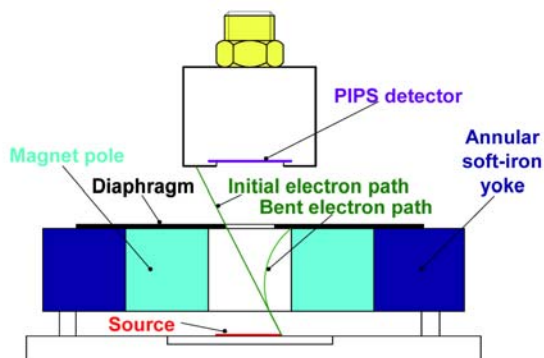


Fig. 7: Bending magnet to deflect conversion electrons from the detector (top). Background and low-energy side of a ^{237}Np - ^{233}Pa spectrum, before and after installing the magnet (bottom).

source and the detector to prevent conversion electrons from reaching the detector (Fig. 7).³¹

3. 2. Applications

Well-resolved spectra on enriched material still contribute to an improvement in the knowledge of nuclear decay data.^{7,31–41} The technique is also used to identify impurities, quantify isotopic compositions or to determine activity ratios between different radionuclides,^{42–49} e.g. for safeguards and nuclear material management. It has also yielded more indirect information, such as e.g. the $^{235}\text{U}/^{238}\text{U}$ half-life ratio using the $^{235}\text{U}/^{234}\text{U}$ activity ratio in the spectra of well characterised ^{235}U -enriched materials as a probe (see Fig. 8).⁵⁰

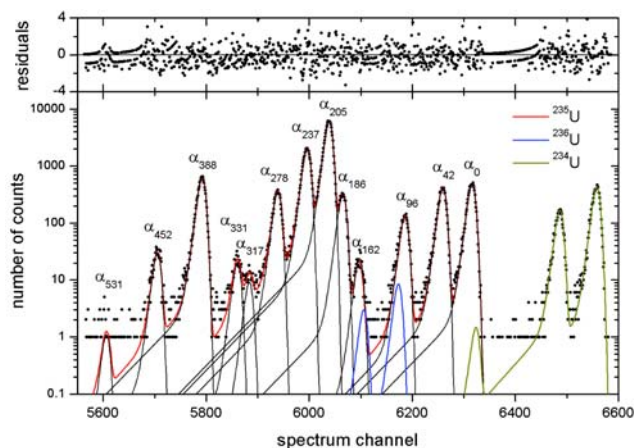


Fig. 8: High-resolution spectrum of ^{235}U with traces of $^{234,236}\text{U}$, revealing nuclear decay data such as emission probabilities, energies and, indirectly, also half-lives.

3. 3. Qualitative Source Preparation

As the application of high-resolution spectrometry usually doesn't require sources with a well-defined quantity of material, one can apply source preparation techniques that deliver better quality with respect to thickness



Fig. 9: Compact vacuum evaporation/sublimation cell with mask for seven source substrates and tungsten filament.

and homogeneity.^{2,26,27} For this purpose, vacuum sublimation is the preferred technique, but its recovery is quite low. At IRMM, a set-up is built with rather close geometry for the simultaneous production of seven sources instead of one (see Fig. 9).

3. 4. Peak Fitting

A limitation of alpha-particle spectrometry arises from spectral interference caused by the presence of nuclides with near identical alpha-emissions, which appear as unresolved or partially resolved multiplets in the measured energy spectrum. Consequently, an accurate determination of individual peak areas cannot be determined by a simple integration method and requires elaborate modelling of the spectrum. Physical processes that determine the peak shape in a silicon detector have been scrutinised.^{51–53} Energy loss, mainly in the solid source, can create significant spectral shifts and additional tailing. The energy spectrum can also be distorted by pile-up effects at elevated count rates, by true coincidences with other emitted particles, such as conversion electrons, or by satellite peaks from recoils implanted in the detector.²⁵

In quasi-ideal measurement conditions, involving thin radioactive sources, small detectors and relatively high source-detector distances, the peak shape can be adequately represented by the convolution of a Gaussian with up to three exponentials, leading to the following analytical function for the spectrum generated by one radionuclide (see also Fig. 8):^{54,55}

$$f(u) = A \sum_{k=1}^n \frac{I_k}{3} \left\{ \sum_{i=1}^3 \left[\frac{\eta_i}{\eta_{\text{tot}}} \frac{1}{\tau_i} \right] \exp \left(\frac{u - \mu_k}{\tau_i} + \frac{\sigma^2}{2\tau_i^2} \right) \operatorname{erfc} \left(\frac{1}{\sqrt{2}} \left(\frac{u - \mu_k}{\sigma} + \frac{\sigma}{\tau_i} \right) \right) \right\} \quad (6)$$

in which A is a measure for the area, I_k is the relative emission probability for peak k , μ_k the peak position, σ the standard deviation of the Gaussian, η_i and τ_i the weight and tailing parameters of exponential i , $\eta_{\text{tot}} = \sum \eta_i$ the total weight and erfc the complementary error function. Similar functions can be added for each additional radionuclide contribution to the spectrum. The relative intensities I_k are constants, whereas the area A varies from one spectrum to another.

The alpha-particle energy spectrum is fitted with home-made least-squares fitting software, such as ALFA or ALPHA, the former being an APL application and the latter a spreadsheet application.^{55–57} In principle, the uncertainty on the fitted parameters follows from the covariance matrix.⁵⁸ In practice, one finds that fit programs seem to underestimate the uncertainty on fitted variables. In the field of half-life measurements,

there is well-documented proof of underestimation of the uncertainty on the fitted half-life value to activity measurements, in particular if the residuals of the fit are auto-correlated.⁵⁹ There are also known bias effects when fitting Poisson distributed data, the sign and magnitude depending on the choice of statistical weight.⁶⁰ If the spectral decomposition is not too complicated, one can opt to take the numerical integral in the peak region and make separate corrections for tailing effects.⁶¹

3. 5. Off-line Gain Stabilisation

As high-resolution alpha-particle spectrometry sometimes requires long measurement times to obtain sufficient statistical accuracy, electronic gain shift can significantly influence the overall resolution. An off-line gain stabilisation method has been developed to quantify and counteract gain shifts in subsequent spectra or in a data stream.^{62,63}

The human eye recognises gain shifts by the displacement of spectral features (peaks, valleys) with respect to their position in a previous spectrum, acting as a reference spectrum. Mathematically one can align two spectra e.g. by maximising their mutual convolution. A more convenient way of estimating the shift is based on the Stieltjes integral of a spectrum, $f_{\text{shifted}}(x)$, with respect to the reference spectrum, $f(x)$:⁶³

$$\text{shift} \approx \frac{\int_a^b f_{\text{shifted}}(x) \cdot f'(x) dx - \frac{1}{2} [f(b)^2 - f(a)^2]}{- \int_a^b f'(x)^2 dx \cdot \int_a^b f_{\text{shifted}}(x) dx / \int_a^b f(x) dx} \quad (7)$$

The second term in the numerator is negligible if the integration is performed between two points where the count rate is extremely low, i.e. $f(a) = f(b) = 0$. The alpha-particle spectra are taken with high resolution (8K channels), so that the spectrum $f(x)$ is a continuous and slowly varying function from one channel to the next. The Stieltjes integral combines the number of counts in each channel with the first derivative in the corresponding channel of the reference spectrum. The predominance of counts in channels with a negative $f'(x)$ value is interpreted as a drift in the forward direction, and vice versa. The denominator acts as a normalisation factor, based on the consideration that $f'(x) = f_{\text{shifted}}(x) - f(x)$, if the shift is exactly one channel, i.e. $f_{\text{shifted}}(x) = f(x + 1)$.

If data are collected one-by-one in list mode, the shift can be followed as a function of time and an individual correction can be made for each count. The local shift is then obtained from an exponentially moving average:

$$\text{shift} \approx f'(x) \left[- \int_a^b f(x) dx / \int_a^b f'(x)^2 dx \right] n^{-1} + \text{shift}_{\text{previous}} (1 - n^{-1}) \quad (8)$$

in which n is a number representing the ‘memory range’. A more stable trend line is obtained by analysing the data in the backward as well as the forward direction, as local effects cancel out in the average and global changes are detected with less delay.

Fig. 10 shows a fraction of the summed ^{235}U alpha-particle spectrum, with and without gain shift correction. The best result was obtained with point-by-point shift correction.

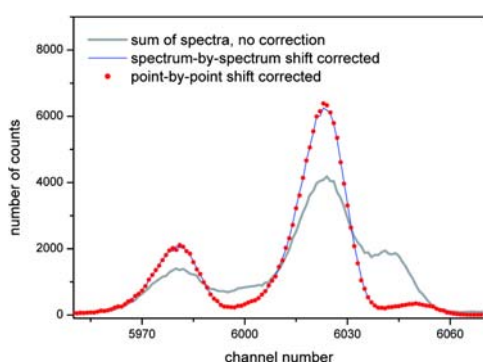


Fig. 10: Detail of a gain-shift corrected and non-corrected sum of 150 alpha spectra (see Fig. 8).

4. Conclusions

Technical aspects concerning the application at IRMM of alpha-particle counting at a defined low solid angle and of high-resolution alpha-particle spectrometry have been discussed. Whereas these techniques are used in the frame of primary standardisations of radioactive solutions or for the determination of nuclear decay data, many of the findings can be transferred to other applications of alpha-particle spectrometry. This includes subjects like source preparation, instrumentation, solid-angle calculations, peak shapes, fitting routines, bias of least-squares methods, off-line stability corrections, simulation of energy loss, uncertainties, etc.

5. References

1. S. Pommé, *Metrologia* **2007**, 44, S17-S26
2. G. Bortels, Status of high-resolution α -particle spectrometry using Si detectors, in: Proceedings of the 13th ESARDA symposium on safeguards and nuclear material management, Avignon, France, 14–16 May **1991**, ESARDA24, EUR 13686 EN, pp. 159–163
3. E. García-Toraño, *Appl. Radiat. Isot.* **2006**, 64, 1273–1280
4. W. Bambynek, Precise solid-angle counting, Standardization of Radionuclides, (IAEA, Vienna, 1967), pp. 373–383
5. A. Spagnol, B. Denecke, Problems and improvements in low geometry alpha counting In: M.L. Hurrell (ed.), Chemical nuclear data (The British Nuclear Energy Society, London, 1971), pp. 199–203
6. B. Denecke, R. Eykens, J. Pauwels, P. Robouch, D. M. Gilliam, P. Hodge, J.R.M. Hutchinson, J.S. Nico, *Nucl. Instr. and Meth.* **1999**, A438, 124–130
7. M. Woods et al., *Appl. Radiat. Isot.*, **2002**, 56, 415–420
8. L. Johansson, T. Altitzoglou, G. Sibbens, S. Pommé, B. Denecke, *Nucl. Instr. Meth.* **2003**, A505, 699–706
9. G. Sibbens, S. Pommé, T. Altitzoglou, *Appl. Radiat. Isot.* **2004**, 61, 405–408
10. A. Spagnol, First results of a new series of measurements for the precise determination of the half lives of ^{234}U and ^{235}U , EANDC-53 “S”, **1966**, pp. 393–398
11. R. Vaninbrouckx, Status report from CBNM-JRC to the second coordinated research meeting on the measurement of transactinium nuclear decay data, in: A. Lorenz (ed.), Second coordinated research meeting on the measurement of transactinium nuclear decay data, IAEA Nuclear Data Section, INDC(NDS)-105-N, Aix-en-Provence, **1979**, pp. 45–48
12. R. Vaninbrouckx, Half-Life of ^{239}Pu : Present Status, in: A. Lorenz (ed.), Second coordinated research meeting on the measurement of transactinium nuclear decay data, IAEA Nuclear Data Section, INDC(NDS)-105-N, Aix-en-Provence, **1979**, pp. 49–50
13. S. Pommé, T. Altitzoglou, R. Van Ammel, G. Sibbens, A. Verbruggen, R. Eykens, J. Camps, K. Kossert, H. Janssen, Eduardo García-Toraño, T. Durán, F. Jaubert, Experimental determination of the U-233 half-life, unpublished
14. G. Sibbens, Silicon charged-particle detectors for alpha-particle spectrometry and alpha-particle counting, Lecture notes for VERMI Young Researchers Workshop, Geel 15–19 November 2004, Internal report IRMM, GE/R/IM/26/04, **2004**
15. S. Pommé, L. Johansson, G. Sibbens, B. Denecke, A new algorithm for the solid angle calculation applied in alpha-particle counting, Internal Report IRMM, GER/RN/08/2001
16. O. Lerch, A. Spagnol, Geometry factors in low and medium geometry solid angle counting EANDC-53 “S”, **1966**, pp. 415–427
17. S. Pommé, *Nucl. Instr. and Meth.* **2004**, A531, 616–620
18. S. Pommé, J. Paepen, *Nucl. Instr. and Meth.* **2007**, A579, 272–274
19. B. Denecke, Numerieke berekening van ruimtehoeken voor complexe geometrische opstellingen van bron en detector in nucleaire metingen, Master thesis, Postuniversitair Centrum Limburg, **1982**
20. S. Pommé, L. Johansson, G. Sibbens, B. Denecke, *Nucl. Instr. Meth.* **2006**, A505, 286–289
21. G. Sibbens, S. Pommé, L. Johansson, B. Denecke, *Nucl. Instr. Meth.* **2003**, A505, 277–281

22. Y. Spasova, S. Pommé, L. Benedik, U. Wätjen, *Act. Chimi. Slo.* **2007**, *54*, 854–858.
23. S. Pommé, Applied Modeling and Computations in Nuclear Science. T.M. Semkow, S.Pommé, S.M. Jerome, and D. J. Strom, Eds. ACS Symposium Series 945. American Chemical Society, Washington, DC, 2006, ISBN 0-8412-3982-7, pp. 218–233
24. S. Pommé, Cascades of pile-up and dead time, *Appl. Radiat. Isot.*, in press
25. A. Nylandsted Larsen, G. Bortels, B. Denecke, *Nucl. Instr. Meth.* **1984**, *219*, 339–346
26. G. Sibbens, Overview of source preparation techniques applied to primary standardisation. Lecture notes for VERMI Young Researchers Workshop, Paris 1–5 December 2003, Internal Report IRMM, GE/IM/40/2003/11/24, **2003**
27. G. Sibbens, T. Altitzoglou, *Metrologia* **2007**, *44*, S71–S78
28. BIPM Mass Certificate no. 65, 1 kg mass standard in stainless steel IRMM-15918, **2002**
29. B. Denecke, G. Sibbens, T. Szabo, M. Hult, L. Persson, *Appl. Radiat. Isot.* **2000**, *52*, 351–355
30. S. Pommé, C. Wagemans, F. Verhaegen, L. Van Den Durpel, J. Van Gils, R. Barthélémy, *Nucl. Instr. and Meth.* **1995**, *A 359*, 587–595
31. G. Sibbens, B. Denecke, *Appl. Radiat. Isot.* **2000**, *52*, 467–470
32. G. Bortels, B. Denecke, R. Vaninbroux, *Nucl. Instr. and Meth.* **1984**, *223*, 329–335
33. G. Bortels, D. Reher, R. Vaninbroux, *Appl. Radiat. Isot.* **1984**, *35*, 305–310
34. R. Vaninbroux, G. Bortels, B. Denecke, *Appl. Radiat. Isot.* **1984**, *35*, 1081–1087
35. R. Vaninbroux, G. Bortels, B. Denecke, *Appl. Radiat. Isot.* **1986**, *37*, 1167–1172
36. G. Bortels, D. Mouchel, R. Eykens, E. García-Toraño, M. L. Aceña, R.A.P. Wiltshire, M. King, A. J. Fudge, P. Burger, *Nucl. Instr. and Meth.* **1990**, *A295*, 199–206
37. E. García-Toraño, M. L. Aceña, G. Bortels, D. Mouchel, *Nucl. Instr. and Meth.* **1992**, *A 312*, 317–322
38. G. Bortels, D. Mouchel, García-Toraño, M. L. Aceña, *Appl. Radiat. Isot.* **1992**, *43*, 247–252
39. E. García-Toraño, M. L. Aceña, G. Bortels, D. Mouchel, *Nucl. Instr. and Meth.* **1993**, *A334*, 477–484
40. G. Sibbens, S. Pommé, *Appl. Radiat. Isot.* **2004**, *60*, 155–158
41. E. García-Toraño, M. T. Crespo, M. Roteta, G. Sibbens, S. Pommé, A. Martín Sánchez, M. P. Rubio Montero, S. Woods, A. Pearce, *Nucl. Instr. and Meth.* **2005**, *A550*, 581–592
42. G. Bortels, I. L. Barnes, P. De Bièvre, K.M. Glover, Characterization of the AS-76 samples, The AS-76 interlaboratory experiment on the alpha spectrometric determination of Pu-238, Part III: Preparation and Characterisation of Samples, KfK 2862, EUR 6402e, **1979**, pp. 14–23
43. G. Bortels, AS-76 characterization by alpha particle spectrometry at CBNM, Geel, The AS-76 interlaboratory experiment on the alpha spectrometric determination of Pu-238, Part III: Preparation and Characterisation of Samples, KfK 2862, EUR 6402e, **1979**, pp. 24–36
44. G. Bortels, P. De Bièvre, L. Barnes, K.M. Glover, Characterization of the samples used in the AS-76 interlaboratory experiment on the determination of ^{238}Pu , Publication service of the JRC, Ispra, **1979**, pp.380–387
45. G. Bortels, Determination of the α -activity ratio ^{228}Th – ^{232}U in the Harwell spike solution used in the USIP phase III, Report on the second Uranium-Series intercomparison project workshop, Harwell, 24–25 June 1980, AERE-R 10044, **1981**, pp. 34–38
46. G. Bortels, A. Verbruggen, Accurate measurement of the ^{238}Pu -activity fraction in the NBS plutonium SRM 946 and 947, in: L. Stanchi (ed.), Proceedings of the 6th ESARDA symposium on safeguards and nuclear material management, Venice, Italy, **1984**, pp. 431–432
47. G. Bortels, A. Verbruggen, G. Sibbens, T. Altitzoglou, EU-ROMET Project No 325: Analysis of Plutonium Alpha-Particle Spectra, Internal Report IRMM, GE/R/RN/01/96, **1996**
48. T. Altitzoglou, G. Sibbens, M. Bickel, A. Bohnstedt, J.-G. Decaillon, C. Hill, L. Holmes, *Appl. Radiat. Isot.* **2004**, *61*, 395–399
49. G. Sibbens, T. Altitzoglou, S. Pommé, R. Van Ammel, α -particle and γ -ray spectrometry of a plutonium solution for impurity determination, *Appl. Radiat. Isot.*, in press
50. S. Pommé, E. García-Toraño, G. Sibbens, S. Richter, R. Wellum, A. Stolarz, A. Alonso, *J. Radioanal. Nucl. Chem.* **2008**, *277*, 207–210.
51. E. Steinbauer, G. Bortels, P. Bauer, J. P. Biersack, P. Burger, I. Ahmad, *Nucl. Instr. and Meth.* **1994**, *A 339*, 102–108
52. E. Steinbauer, P. Bauer, M. Geretschläger, G. Bortels, J. P. Biersack, P. Burger, *Nucl. Instr. and Meth.* **1994**, *B85*, 642–649
53. P. Bauer, G. Bortels, *Nucl. Instr. and Meth.* **1990**, *A299*, 205–209
54. G. Bortels, P. Collaers, *Appl. Radiat. Isot.*, **1987**, *38*, 831–837
55. G. Bortels, C. Hurtgen, D. Santry, *Appl. Radiat. Isot.*, **1995**, *46*, 1135–1144
56. G. Bortels, D. Mouchel, E. García-Toraño, M. L. Aceña, *Nucl. Instr. and Meth.* **1990**, *A 286*, 429–432
57. T. Babeliowsky, G. Bortels, *Appl. Radiat. Isot.* **1993**, *44*, 1349–1358
58. G. Sibbens, *Appl. Radiat. Isot.*, **1998**, *49*, 1241–1244
59. S. Pommé, Applied Modeling and Computations in Nuclear Science. T. M. Semkow, S. Pommé, S. M. Jerome, and D. J. Strom, Eds. ACS Symposium Series 945. American Chemical Society, Washington, DC, 2006, ISBN 0-8412-3982-7, pp. 282–292
60. S. Pommé, J. Keightley, Applied Modeling and Computations in Nuclear Science. T. M. Semkow, S. Pommé, S. M. Jerome, and D. J. Strom, Eds. ACS Symposium Series 945. American Chemical Society, Washington, DC, 2006, ISBN 0-8412-3982-7, pp. 316–334
61. G. Sibbens; S. Pommé, R. Van Ammel, Total activity and Pu-

- 238/Pu-239+240 ratio by alpha-particle counting and spectrometry for NUSIMEP-5, Internal Report IRMM, GE/R/IM/01/06, 2006
62. S. Pommé, G. Sibbens, *Appl. Radiat. Isot.* **2004**, *60*, 151–154
63. S. Pommé, G. Sibbens, *Advanced Mathematical and Computational Tools in Metrology VI*, ed. P. Ciarlini, M. G. Cox, F. Pavese, G. B. Rossi, *Series on Advances in Mathematics for Applied Sciences – Vol. 66* (World Scientific Publishing Company, 2004) pp. 327–329

Povzetek

V prispevku je opisana uporaba štetja delcev alfa pod določenim majhnim prostorskim kotom in visokoločljivostna spektrometrija alfa v laboratorju za primarno standardizacijo na inštitutu IRMM. Tehniko uporabljamo tako za meritve pri standardizaciji radioaktivnih izvorov kakor tudi za določitev jedrskih karakteristik (delež razpada alfa, razpolovni čas, itd.). V prispevku so podrobno predstavljeni uporabljena instrumentacija in različni postopki pri opisani tehniki, kot so priprava vzorcev, računanje prostorskega kota, ovrednotenje površine vrha, odstopanje merilnih rezultatov, korekcije stabilnosti in izračun merilne negotovosti. Predstavljeni algoritmi niso uporabni samo pri meritvah v sklopu primarne standardizacije, pač pa so uporabni tudi pri rutinskih alfa spektrometričnih meritvah, predvsem pri oceni merilne negotovosti.